

DISTRIBUTION IN MICE OF $^{99m}\text{Tc(V)-DMSA}$ AND $^{188}\text{Re(V)-DMSA}$

ANTIOCO FRANCO SEDDA, GABRIELE ROSSI

ENEA – Unità Tecnica Tecnologie dei Materiali
Laboratorio Tecnologie di Irraggiamento
Centro Ricerche Casaccia, Roma

CESIDIO CIPRIANI

Divisione di Medicina Nucleare, Istituto AIGa, L'Aquila

GIAMPIERO ATZEI, SERGIO BOEMI

Reparto di Medicina Nucleare, Ospedale S. Eugenio, Roma

MAURIZIO MATTEI

Dipartimento di Biologia, Stazione per la Tecnologia Animale
Università di Tor Vergata, Roma



AGENZIA NAZIONALE PER LE NUOVE TECNOLOGIE,
L'ENERGIA E LO SVILUPPO ECONOMICO SOSTENIBILE

DISTRIBUTION IN MICE OF $^{99m}\text{Tc(V)}$ -DMSA AND $^{188}\text{Re(V)}$ -DMSA

ANTIOCO FRANCO SEDDA, GABRIELE ROSSI

ENEA – Unità Tecnica Tecnologie dei Materiali
Laboratorio Tecnologie di Irraggiamento
Centro Ricerche Casaccia, Roma

CESIDIO CIPRIANI

Divisione di Medicina Nucleare, Istituto AIGa, L'Aquila

GIAMPIERO ATZEI, SERGIO BOEMI

Reparto di Medicina Nucleare, Ospedale S. Eugenio, Roma

MAURIZIO MATTEI

Dipartimento di Biologia, Stazione per la Tecnologia Animale
Università di Tor Vergata, Roma

I Rapporti tecnici sono scaricabili in formato pdf dal sito web ENEA alla pagina
<http://www.enea.it/it/produzione-scientifica/rapporti-tecnici>

I contenuti tecnico-scientifici dei rapporti tecnici dell'ENEA rispecchiano l'opinione degli autori e non necessariamente quella dell'Agenzia.

The technical and scientific contents of these reports express the opinion of the authors but not necessarily the opinion of ENEA.

DISTRIBUTION IN MICE OF $^{99m}\text{Tc(V)}$ -DMSA AND $^{188}\text{Re(V)}$ -DMSA

ANTIOCO FRANCO SEDDA, GABRIELE ROSSI, CESIDIO CIPRIANI, GIAMPIERO ATZEI, SERGIO BOEMI
MAURIZIO MATTEI

Abstract

The complex $^{99m}\text{Tc(V)}$ -DMSA has been adopted as imaging agent in medullary thyroid carcinoma but it is also useful in imaging other soft tissue and bone tumors, particularly osseous metastases.

The preparation of $^{188}\text{Re(V)}$ -DMSA can generally be carried out by similar methods, providing a potentially therapeutic radiopharmaceutical for bone tumours. A series of one-pot preparations of $^{99m}\text{Tc(V)}$ -DMSA and of $^{188}\text{Re(V)}$ -DMSA has been carried out in our laboratories, in order to optimize the labelling yield. In a series of animal experiments, mice OUTBRED CD1 were injected with preparations of $^{99m}\text{Tc(V)}$ -DMSA and of $^{188}\text{Re(V)}$ -DMSA, and whole-body planar scintigraphy scans was obtained. After scintigraphic scans, the organs were removed and their radioactivity counted; autoradiography of thin layers of selected organs have also been performed. The data obtained will be the starting point for the preparation of a clinical trial aimed at the diagnosis and palliation of patients with dolorous bone metastases from prostatic cancer by using $^{99m}\text{Tc(V)}$ -DMSA and $^{188}\text{Re(V)}$ -DMSA.

Keywords: $^{99m}\text{Tc(V)}$ -DMSA, $^{188}\text{Re(V)}$ -DMSA, bone metastases, scintigraphy.

Riassunto

Il complesso $^{99m}\text{Tc(V)}$ -DMSA è stato adottato come agente di imaging nel carcinoma midollare della tiroide, ma è utile anche nell' imaging di tumori dei tessuti molli e ossei, in particolare metastasi ossee. La preparazione di $^{188}\text{Re(V)}$ -DMSA può essere generalmente eseguita con metodi simili, fornendo un radiofarmaco potenzialmente terapeutico per tumori ossei. Una serie di preparazioni a singolo stadio di $^{99m}\text{Tc(V)}$ -DMSA e di $^{188}\text{Re(V)}$ -DMSA è stata effettuata nei nostri laboratori, al fine di ottimizzare la resa di marcatura. In una serie di esperimenti su animali, alcuni topi outbred CD1 sono stati iniettati con preparazioni di $^{99m}\text{Tc(V)}$ -DMSA e di $^{188}\text{Re(V)}$ -DMSA, e scansioni planari scintigrafiche whole body sono state ottenute. Dopo le scansioni scintigrafiche gli organi sono stati rimossi e le loro radioattività sono state contate; sono state anche ottenute autoradiografie di strati sottili di organi selezionati. I dati ottenuti saranno il punto di partenza per la preparazione di uno studio clinico finalizzato alla diagnosi e palliazione mediante $^{99m}\text{Tc(V)}$ -DMSA e $^{188}\text{Re(V)}$ -DMSA di pazienti con metastasi ossee dolorose da tumore prostatico.

Parole chiave: $^{99m}\text{Tc(V)}$ -DMSA, $^{188}\text{Re(V)}$ -DMSA, metastasi ossee, scintigrafia.

Index

Introduction 7

Materials and methods 11

Results..... 12

Discussion..... 21

References 24

Introduction

The complex $^{99m}\text{Tc(V)}\text{-DMSA}$ has been adopted as imaging agent in medullary thyroid carcinoma (1,2), but has shown to be also useful in imaging other soft tissue tumors (3-9), osteosarcoma and bone metastases (10-13).

The normal uptake of $^{99m}\text{Tc(V)}\text{-DMSA}$ is seen in nasal mucosa, female breasts, blood pool activity (3 h) and kidneys. It is also actively uptaken by the growth plates of the growing bones, as evidenced in a number of pediatric age group; the blood pool activity seen in the 3 h images is not evident in the 24 h images. Preferential uptake of $^{99m}\text{Tc(V)}\text{-DMSA}$ in malignant lesions and in highly recurrent benign lesion has been reported, similarly to high uptake of fluorine-18-FDG, and generally represents viability of malignant tumors (14). The uptake of the tracer in the case of bone metastases shows, particularly in prostate cancer metastases, an high target/non target ratio. The metastasis of prostate cancer to bone is the most significant cause of morbidity and mortality in this disease, and about 30 000 men/year die due to prostate cancer bone metastasis (15). Current treatments increase survival of 2 months; bisphosphonates are often the only treatment offered to patients, only for palliative purposes. The prostate cancer metastases produce lesions that are typically found near red bone marrow and result in osteoblastic lesion with new woven bone forming on medullary trabeculae. In addition, evidence from pathology reports indicates that this osteoblastic lesion often forms on an area of previous osteolysis.

The exact mechanism of $^{99m}\text{Tc(V)}\text{-DMSA}$ accumulation in tumours, bones and bone metastases is basically unclear. According different hypotheses the tracer is believed to be taken up by tumour cells, or by osteocytes in the early phase of the healing bone reaction, or by the inorganic Ca-P bone matrix. The fixation of $^{99m}\text{Tc(V)}\text{-DMSA}$ in bone has been demonstrated in metastases originated from prostate, breast, melanoma, osteosarcoma, lung, Ewing's sarcoma, rhabdomyosarcoma, papillary and follicular thyroid carcinoma and fibrous dysplasia. This fact strongly suggest that the fixation on the metastases is independent from the primary tumor, and is rather related to a mechanism in the destruction/rebuilding of osseous structure. It was also demonstrated that $^{99m}\text{Tc(V)}\text{-DMSA}$ utilizes the type III NaPi co-transporters, as phosphonoformic acid, a competitive inhibitor of NaPi co-transport, strongly affects $^{99m}\text{Tc(V)}\text{-DMSA}$ uptake (16), and studies have suggested that DMSA V transport is analogous to phosphate transport in cancer cells (17,18).

Other studies showed that different lines of human breast cancer and prostate cancer have also a direct $^{99m}\text{Tc(V)}\text{-DMSA}$ uptake inversely related to cell density (19,20), and it has been suggested, on the basis of the study of a single patient, that uptake of

the tracer is not only due to bone remodeling, but also to the tumor itself, or to the associated inflammatory cells (21).

The structure of the Ca–P solid phase in bone was identified by X-ray diffraction as a crystalline calcium phosphate similar to geological apatite; the bone crystals were found to contain significant and varying amounts of carbonate and HPO_4^{2-} ions, and the biological bone apatites contain only a very small percentage of the total number of hydroxyl groups present in highly purified synthetic calcium hydroxyapatites. The chemical composition, particle size and degree of crystallinity of the single bone crystals is a significant function of the age of the crystal, defined as the elapsed time between the initial deposition of the crystals, directly related to the local turnover of bone substance (22). The composition of biological apatites is very complex; in some cases a replacement of the PO_4^{3-} anions by bivalent species, HPO_4^{2-} and CO_3^{2-} occurs, which have also been detected in large and variable amounts in samples of bone mineral; the initial solid phase of Ca–P formed during the calcification of bone is a poorly crystalline apatite or an amorphous Ca–P, only later replaced by crystalline apatite (23-26). The calcium of nanocrystalline apatite can be replaced by magnesium (up to 8.5%) or strontium (up to 20%), and HPO_4^{2-} ions can be exchanged by carbonate, up to 44%, with minor changes in the X-ray diffraction patterns and its crystal appearance (27).

In a mouse model of metastasis-bearing bones from prostate cancer cells it has been demonstrated that carbonate substitution was significantly increased in bone lesions, while there was a marked reduction in the level of collagen mineralization and mineral crystallinity (28).

An hypothesis based on the metal-complex equilibrium has suggested the pH sensitive character of $^{99\text{m}}\text{Tc(V)-DMSA}$; this pH dependent shift property is inferred as one of the factors relevant to the accumulation of the complex in neoplastic cells. It is currently a well-established notion that malignant tumors are more acidic than normal tissues, and, as a consequence, a tracer with a selective accumulation in acid tissue can be considered of great interest for a possible therapeutic exploitation (29).

The binding of $^{99\text{m}}\text{Tc(V)-DMSA}$ to amorphous and crystalline tri-calcium phosphates and hydroxyapatites samples was studied in comparison with $^{99\text{m}}\text{Tc-HDP}$ under various sets of conditions. It was demonstrated by autoradiography that $^{99\text{m}}\text{Tc(V)-DMSA}$ has the highest affinity for cortical bone rather than medullar, and that binding was inhibited in the presence of phosphate and was stronger at lower pH; the binding of $^{99\text{m}}\text{Tc(V)-DMSA}$ is different for different mineral chemical compositions, and shows a variation with pH of the exchange solution. Different minerals with the same gross hydroxyapatite nominal composition showed a different exchange capacity for $^{99\text{m}}\text{Tc(V)-DMSA}$. In one case a hydroxyapatite sample changed its

binding from 70% to 35% of the DMSA-complex when the pH shifted from 7.4 to 6, while the ^{99m}Tc -HDP is always strongly bound to the bone mineral analogues across the same pH range studied (30).

The functional groups of hydroxyapatite consist of positively charged pairs of calcium ions and of negatively charged oxygen atoms associated with triplets of crystal phosphates, in a fixed pattern on the crystal surface. Three distinct mechanisms of retention can be identified in the crystals : cation exchange with phosphate ions, anion exchange with calcium ions, and formation of coordination complex with calcium sites (31).

The binding capacity for $^{99m}\text{Tc(V)}$ -DMSA complex has been demonstrated (30) to decrease with increasing pH; as in an anion exchange mechanism an increase of pH of the solution would increase retention of the molecule on Ca^{2+} sites by increasing the negative charge on carboxyl groups, a different mechanism should be involved in this case. The complex binding at acidic and neutral pH is likely dominated by formation of metal coordination complexes between calcium sites and carboxyl group on DMSA molecule; DMSA complex is not appreciably released from hydroxyapatite by the action of human serum or NaCl, but this elution can be obtained by phosphate solutions, that possess a stronger affinity for calcium coordination sites. An in vitro investigation on osteoblast and osteoclast cells were performed, and the comparative affinity of $^{99m}\text{Tc(V)}$ -DMSA and Tc- diphosphate was screened under different acidification conditions. The studies performed on isolated bone cells revealed for $^{99m}\text{Tc(V)}$ -DMSA a very high and specific affinity for osteoclastic cells, with a linear increase in cellular uptake in response to an acid pH environment; the cell culture, with an incubation period at pH 6.2, doubled the uptake of the tracer respect to incubation at pH 7.4.

Autoradiography and enzyme histochemical studies performed in the rat revealed the in-vivo accumulation of $^{99m}\text{Tc(V)}$ -DMSA in areas rich in OC cells; participation of bone cells in the skeletal accumulation of $^{99m}\text{Tc(V)}$ -DMSA was clearly demonstrated (32).

About the possible mechanism of such accumulation, it has been reported that OC cells can be transformed from a non-resorbing to a resorbing state by transferring them to medium at pH 6.5 (33), and the pH decrease might be related to activation of the osteoclastic cells to an activated resorbing state. In this state, after the migration to the resorption site and its attachment to bone, the osteoclast cell undergoes polarization and formation of a new membrane domain, used for attachment of a cell sealing zone to the bone matrix (ruffled border). Dissolution of hydroxyapatite takes place by secretion of HCl through the ruffled border into the resorption lacuna, while several proteolytic enzymes degrade the organic bone matrix. The dissolution process

is followed by removal of all soluble degradation products; after this process osteoclasts undergo either apoptosis or return to their non-resorbing stage.

Lam et al. (30) suggested that the $^{99m}\text{Tc(V)}$ -DMSA complex binding to the bone is mediated by the mineral component hydroxyapatite, while Horiuchi-Suzuki et al. (32) un-ambiguously demonstrated that osteoclast cells are directly involved in internalization of the complex. It is somehow puzzling that both hypotheses are able to explain the attachment of $^{99m}\text{Tc(V)}$ -DMSA to bone, independently from the specific tumor involved, the increase of complex binding with decreasing pH and the direct competition from phosphate ions. $^{99m}\text{Tc(V)}$ -DMSA mimics the behavior of phosphate ions, as the competitive binding data suggest, but the complex, differently from organic phosphonate complexes, shows a negligible binding to healthy bone. The low pH, the increased activity of osteoclast, the presence of free hydroxyapatite nanocrystals, characteristic of lytic bone metastases, strongly increase the binding of the DMSA complex; while its exact binding mechanism still need to be fully clarified, the peculiar chemistry of $^{99m}\text{Tc(V)}$ -DMSA shows great potential as an activity marker of the complex remodeling processes present in bone tumor.

By using the similarities to ^{99m}Tc in preparative and binding chemistry the preparation of $^{188}\text{Re(V)}$ -DMSA can generally be carried out by reduction of Re(VII) to Re(V) by the use of stannous chloride, similarly to the analogue ^{99m}Tc complex, but operating at higher temperature and lower pH. The radioisotope ^{188}Re has been proposed as a suitable candidate for the preparation of radiopharmaceuticals in therapeutic applications, particularly due to its favorable nuclear properties (emission of a beta-particle of 2.2 MeV, $t_{1/2}$ 16.9 h, and a gamma emission of 155 keV. A further advantage comes from the fact that ^{188}Re is conveniently produced from an alumina-based $^{188}\text{W}/^{188}\text{Re}$ generator, and from the presence of gamma emission, that makes possible to conduct post-therapeutic imaging. $^{188}\text{Re(V)}$ -DMSA, the potential therapeutic analogue of the tumour imaging agent $^{99m}\text{Tc(V)}$ -DMSA, has been prepared by one-pot labeling methods; it has also been demonstrated that $^{99m}\text{Tc(V)}$ -DMSA pharmacokinetics and clinical scintigraphic scans are predictive of $^{188}\text{Re(V)}$ -DMSA biodistribution in vivo (34).

This fact can be used to estimate tumour and renal dosimetry and assess the real possibility for patients of a $^{188}\text{Re(V)}$ -DMSA treatment; as this complex is also selectively taken up in bone metastases, it could be a real clinical candidate for palliative treatment of pain associated with this disease. The fact that normal bone is indistinguishable from background soft tissue in both early and delayed images of $^{99m}\text{Tc(V)}$ -DMSA scintigraphic scans is of immense value in dosimetric considerations for minimizing the dose-limiting normal bone marrow toxicity.

In a clinical trial (35) three patients with cancer of the prostate and three with cancer of the bronchus, all with bone metastases, were injected with 370 MBq of

$^{188}\text{Re(V)DMSA}$ and the scintigraphic images were collected at different time intervals.

Organ residence times were estimated from the scans, and used to estimate radiation doses. $^{188}\text{Re(V)DMSA}$ showed selectivity for bone metastases (particularly those from prostate carcinoma) and kidney, but uptake in normal bone was not significantly greater than in surrounding soft tissues. The residence half times for the source organs were 0.47 ± 0.21 h (kidney), 0.52 ± 0.16 h (liver), 0.64 ± 0.48 h (bladder contents) and, 10.44 ± 1.5 h for the remainder of the body. Among the normal tissues the kidneys received the highest radiation dose ($0.5\text{--}1.3$ mGy/MBq), the liver received 0.12 ± 0.04 mGy/MBq and both red marrow and total body received 0.07 ± 0.01 mGy/MBq. It was estimated that with therapeutic, potentially tumouricidal administered activities of 7400 MBq, the renal radiation dose would not be expected to reach the minimum threshold of 1000 cGy, at which radiation nephritis is a risk.

While the preliminary clinical data are quite promising, renal radiation dose might be a matter of concern in a possible high dose therapeutic clinical trial.

Materials and methods

A series of one-pot preparations of $^{99\text{m}}\text{Tc(V)-DMSA}$ has been carried out in our laboratories, by varying DMSA over SnCl_2 ratio, pH, total volume of the solution, in order to minimize the free pertechnetate and to keep the concentration of Tc(III) renal complex as low as possible. The “best” composition was 1.37 mg of DMSA, 8 of NaHCO_3 , 2 mg of Na_2CO_3 , 10 mg of glucose, 0.166 mg of $\text{SnCl}_2\cdot 2\text{H}_2\text{O}$, with a yield of $^{99\text{m}}\text{Tc(V)-DMSA}$ always exceeding 99.8%.

The necessary amount of $^{99\text{m}}\text{Tc-pertechnetate}$ in 2.0 mL of saline for injection was added to the vial, in sterile conditions, at room temperature. The radiochemical purity was determined by TLC on silica gel, with a solvent system n-butanol/ acetic acid/water (3 : 2 : 3 v/v).

A series of one-pot preparations of $^{188}\text{Re(V)-DMSA}$ has also been performed in our laboratory, by varying the reagents ratio, pH and temperature in order to maximize the yield of the product.

The final procedure for the preparation of $^{188}\text{Re(V)-DMSA}$ was as follows: 3 mg of DMSA, 0.3 mg of $\text{SnCl}_2\cdot 2\text{H}_2\text{O}$ and 18 mg of ascorbic acid were dissolved in 0.1 ml of saline; the final pH was 2.0. The mixture was sterilized by $0.22\ \mu\text{m}$ membrane filtration, and 1.0 ml of it was dispensed into pre-sterilized serum vials. The $^{188}\text{W}/^{188}\text{Re}$ generator (ITG Munich, Germany) was eluted with 0.9% saline solution, and the radioactivity assayed using a dose calibrator. 0.5 milliliter of perrhenate

solution (1400 MBq/ml) was added to a vial containing the DMSA solution. The reaction was allowed to proceed 30 min at 92 °C.

The radiochemical purity was determined by silica gel thin layer chromatography (TLC-SG, Merck) employing as mobile phase acetone. R_f : ReO₂ 0.0, ReO₄ 0.9±1.0, ¹⁸⁸Re(V)-DMSA 0.9±1.0) and 0.9% saline solution, R_f : ReO₂ 0.0, ReO₄ 0.9±1.0, ¹⁸⁸Re-DMSA 0.0). The radionuclide purity was verified by gamma ray spectroscopy after suitable decay periods, and the radiochemical stability of the rhenium complex was evaluated 24 h after preparation by TLC-SG.

The final yield of ¹⁸⁸Re(V)-DMSA was greater than 98.5%, without an intermediate purification step, and always demonstrated an excellent stability to radiolysis.

Female mice OUTBRED CD1 with age of 14 weeks were used in all animal experiments, performed in accordance with national regulations regarding animal care and handling, and under ethical committee supervision

200 to 300 microliters of radiopharmaceuticals, each containing 15 to 22 MBq of ^{99m}Tc or ¹⁸⁸Re labelled radiopharmaceutical were injected into the ocular plexus of the mice; each animal weighed 30 g ± 3. Biodistributions were obtained by sacrificing the mice at various times post-injection, and performing whole-body planar scintigraphy scans by using a L'ACN 3 mm pinhole gamma camera, acquiring a total of 100 000 counts.

After scintigraphic scans the organs were removed, weighed, and their radioactivity were counted in a pre-calibrated NaI(Tl) detector system. All sample counts were corrected for background and physical decay; the uptake in each organ was calculated and expressed as percentage of the injected activity per gram and/or as percentage of the injected activity/organ. Autoradiography of thin layers of selected organs have been obtained by using a Cyclone Perkin Elmer image phosphor screen apparatus.

Results

The Figure 1 shows a typical scintigraphic distribution of ^{99m}Tc in the form of pertechnetate. 200 microliters containing 600 microCi of ^{99m}Tc were injected in the ocular plexus, and scintigraphy was obtained 3 h after injection. As expected, the tracer was fixed in thyroid, and mainly eliminated by urinary excretion.

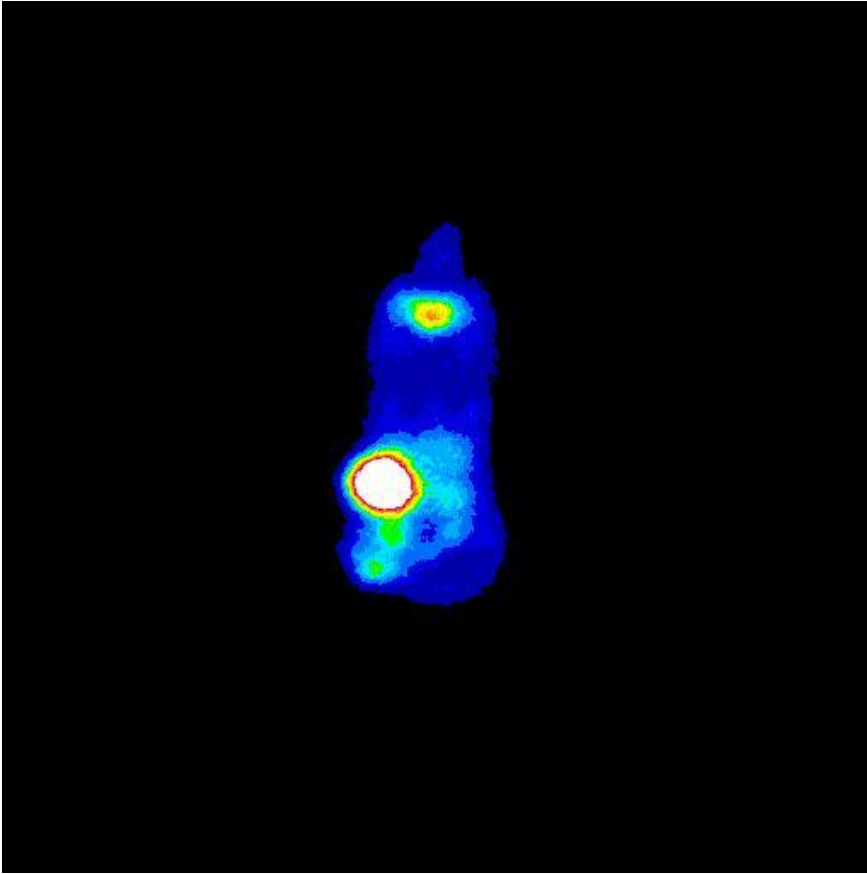


Figure 1

The Figure 2 shows a typical scintigraphic distribution of $^{99m}\text{Tc}(\text{V})$ -oxidronate (hydroxymethylene diphosphonate), a tracer used as a skeletal imaging agent to delineate areas of abnormal osteogenesis. 200 microliters containing 600 microCi of the tracer were injected in the ocular plexus, and scintigraphy was obtained 3 h after injection.

The tracer was fixed in bone (spine, skull and legs are clearly visible), but the mean activity in organs like liver, kidneys and blood was low, as expected.

It is generally accepted that technetium ^{99m}Tc -oxidronate localizes on the surface of hydroxyapatite crystals by a process termed chemisorption, with blood flow and/or blood concentration being most important in the delivery of the agent to sites of uptake. Visualization of osseous lesions is possible since skeletal uptake of ^{99m}Tc -oxidronate is altered in areas of abnormal osteogenesis. It is well known from clinical practice that the binding of the tracer is significantly more extensive where the bone formation activity (osteoblast function) is increased, but its fixation is always present in healthy bone in the whole skeleton.

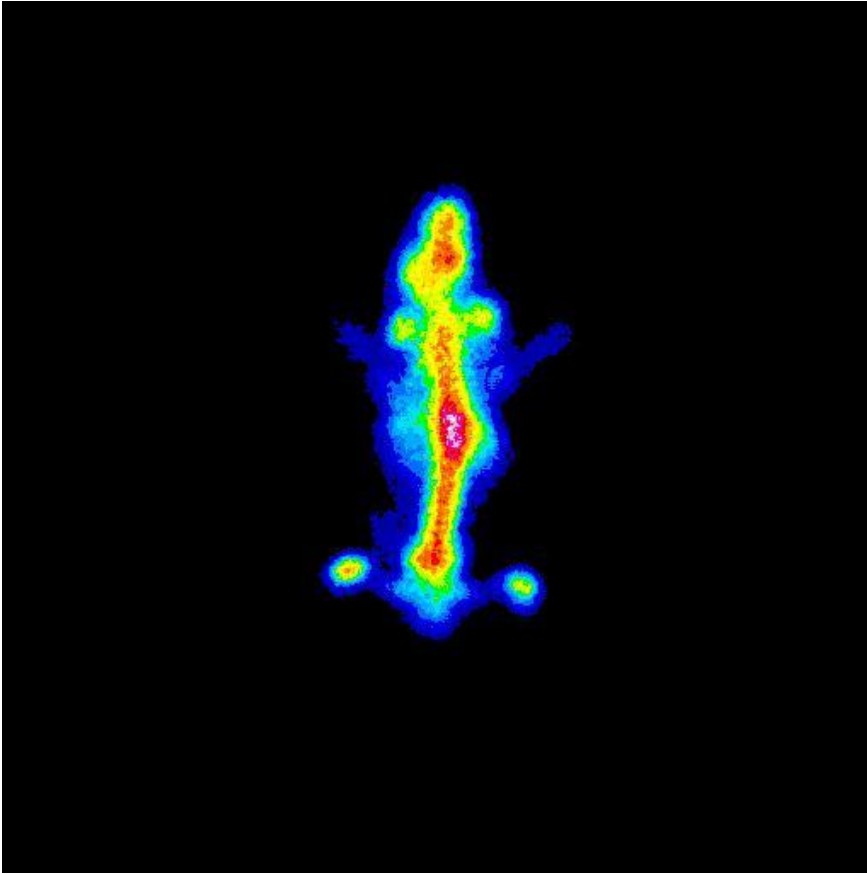


Figure 2

The Figure 3 shows a typical scintigraphic distribution of $^{99m}\text{Tc(V)}$ -DMSA in group A. 200 microliters containing 300 microCi of $^{99m}\text{Tc(V)}$ -DMSA were injected in the ocular plexus, and scintigraphy was obtained 3 h after injection. As expected, the tracer is fixed in bone (spine and skull are clearly visible), in kidneys and, marginally, in liver.

On 12 animals the total radioactivity distribution 3 h p.i. has been:

<i>ORGAN</i>	<i>% of TOTAL RADIOACTIVITY</i>
bladder	89% \pm 3%
kidneys	1.4% \pm 0.2%
liver	1.1% \pm 0.1%
intestines	1.1% \pm 0.1%
Body carcass	7.2% \pm 0.4%

While the specific activity has been

<i>ORGAN</i>	<i>SPECIFIC RADIOACTIVITY (microCurie/g)</i>
kidneys	16.6 ± 2
liver	14.0 ± 2
intestines	6.9 ± 1.5
Body carcass	6.1 ± 1.5

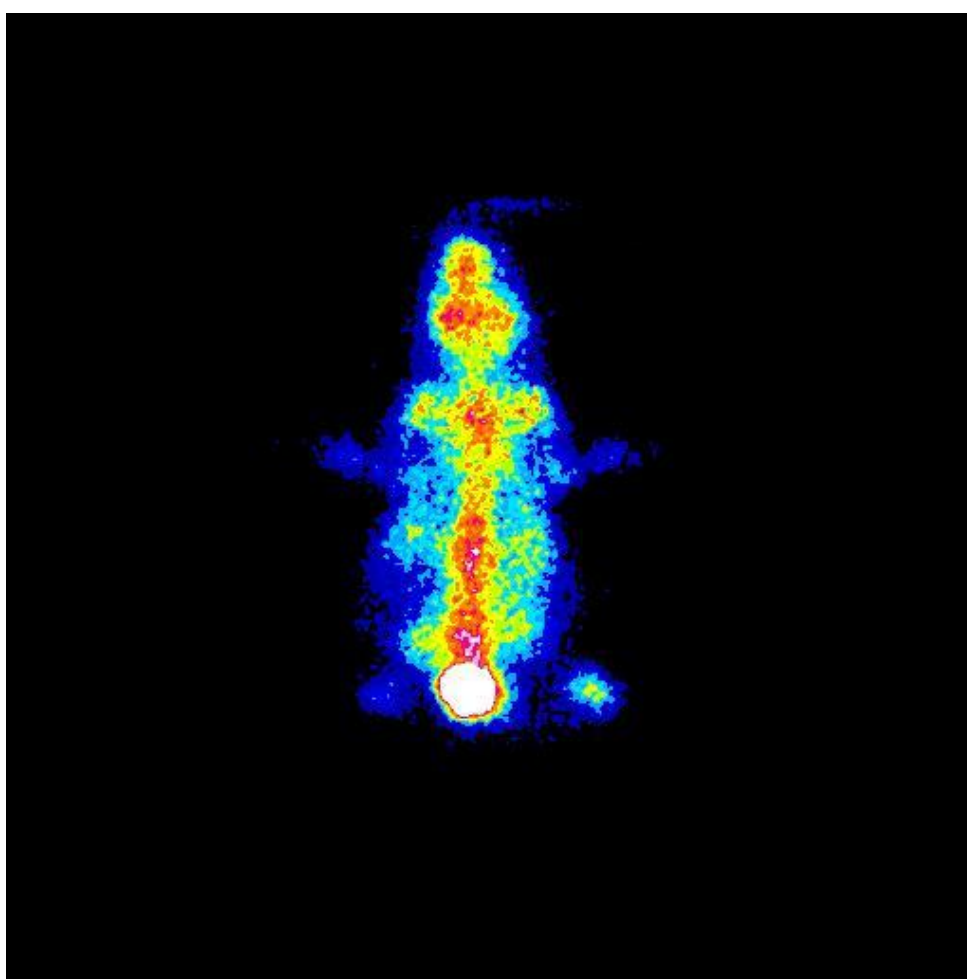


Figure 3

The Figure 4 shows a typical scintigraphic distribution of $^{99m}\text{Tc(V)}$ -DMSA in vivo after 6 h p.i. of 200 microliters containing 600 microCi of $^{99m}\text{Tc(V)}$ -DMSA in the ocular plexus. As visible from the scintigraphy, the tracer is only significantly fixed in kidneys and, marginally, in blood.

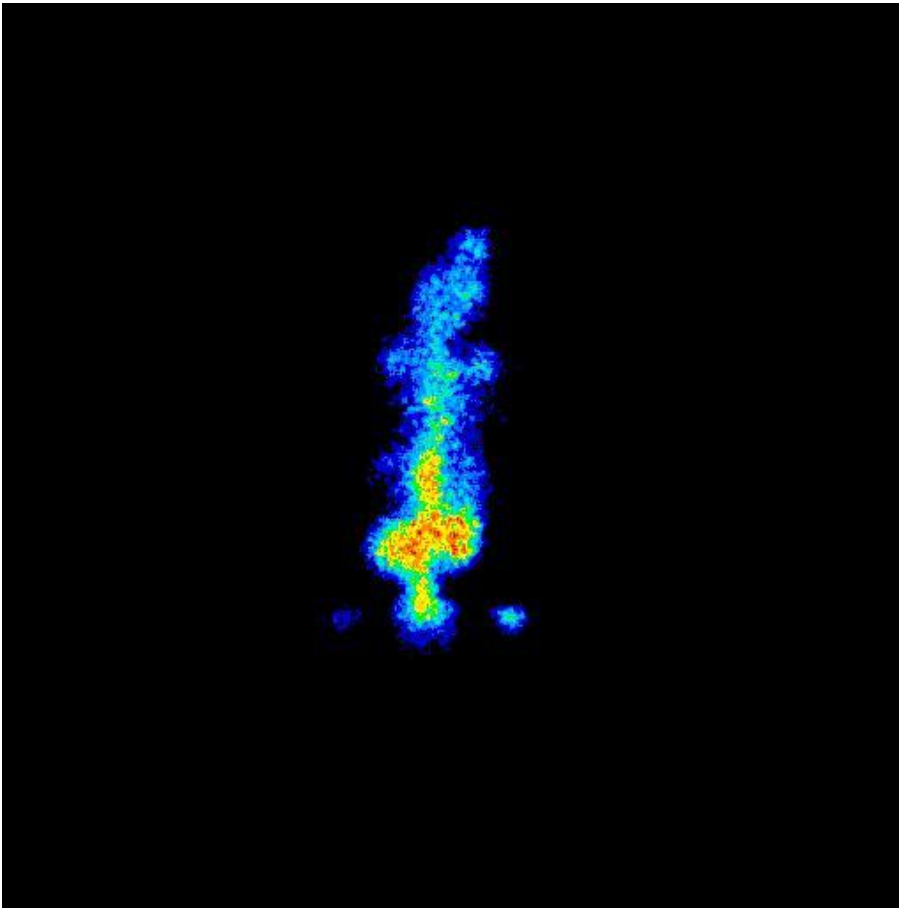


Figure 4

The Figure 5 shows a typical scintigraphic distribution of $^{99m}\text{Tc(V)}$ -DMSA in an animal to which 100 microliters of a solution containing 2 mg of DMSA has been orally administered before the injection. After 1 hour, 200 microliters containing 300 microCi of $^{99m}\text{Tc(V)}$ -DMSA were injected in the ocular plexus, and scintigraphy was obtained 3 h after injection.

The tracer is fixed in bone (spine and skull are also clearly visible), but the mean activity in organs like liver and kidney is lower respect to the animals that have not ingested DMSA. Kidney, in particular, shows an uptake reduced of about 20%.

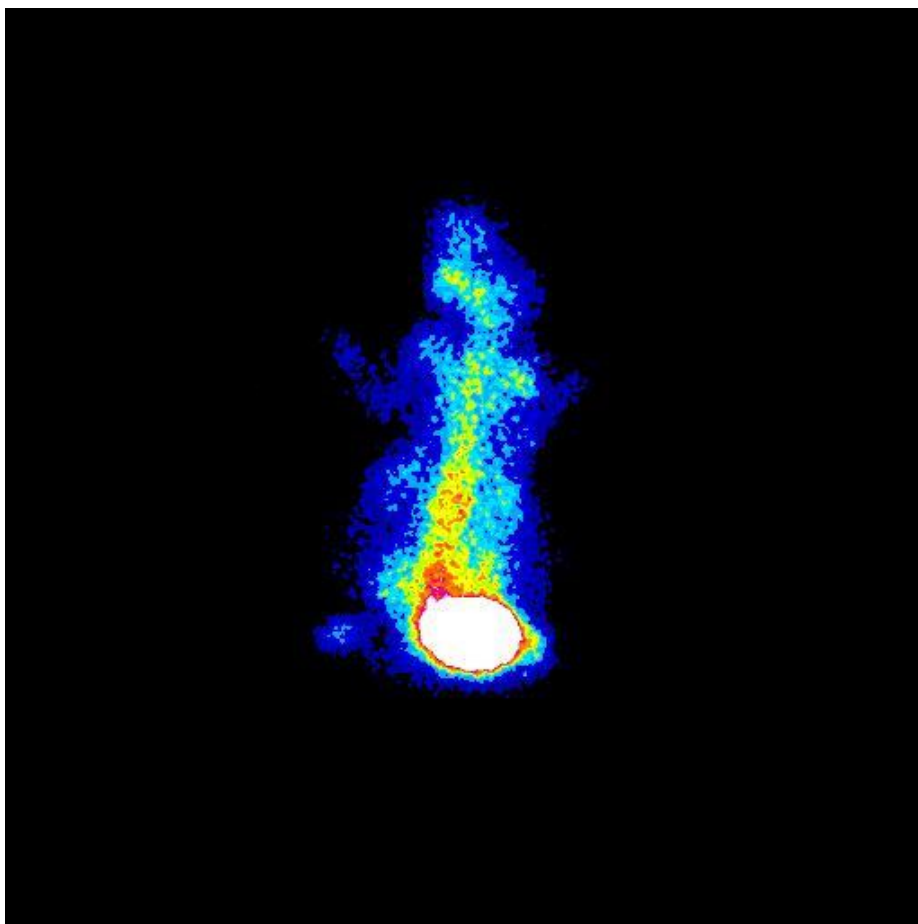


Figure 5

The present data confirm the observation (36) that cold DMSA, injected in rats and rabbits immediately before $^{99m}\text{Tc(V)}$ -DMSA, is able to reduce the renal uptake of the radioactive tracer without significantly reducing the tumor uptake.

The Figure 6 is an autoradiography of a mouse kidney injected with 200 microliters containing 1250 microCurie of $^{188}\text{Re(V)}$ -DMSA; it is clearly visible that the most of the radioactivity is present in the cortical section of the organ. It has been demonstrated (30) that more than 80% of the radioactivity in the cortex was confined to the cytoplasm of renal tubular cells, with some cortical tubule sections showing high grain density in all the constituent cells and others showing low density in all constituent cells, implying that the uptake process occurs only in specific segments of the tubule, as demonstrated in Figure 7, that shows a linear scan plot of the radioactivity distribution along a line transverse to the kidney.

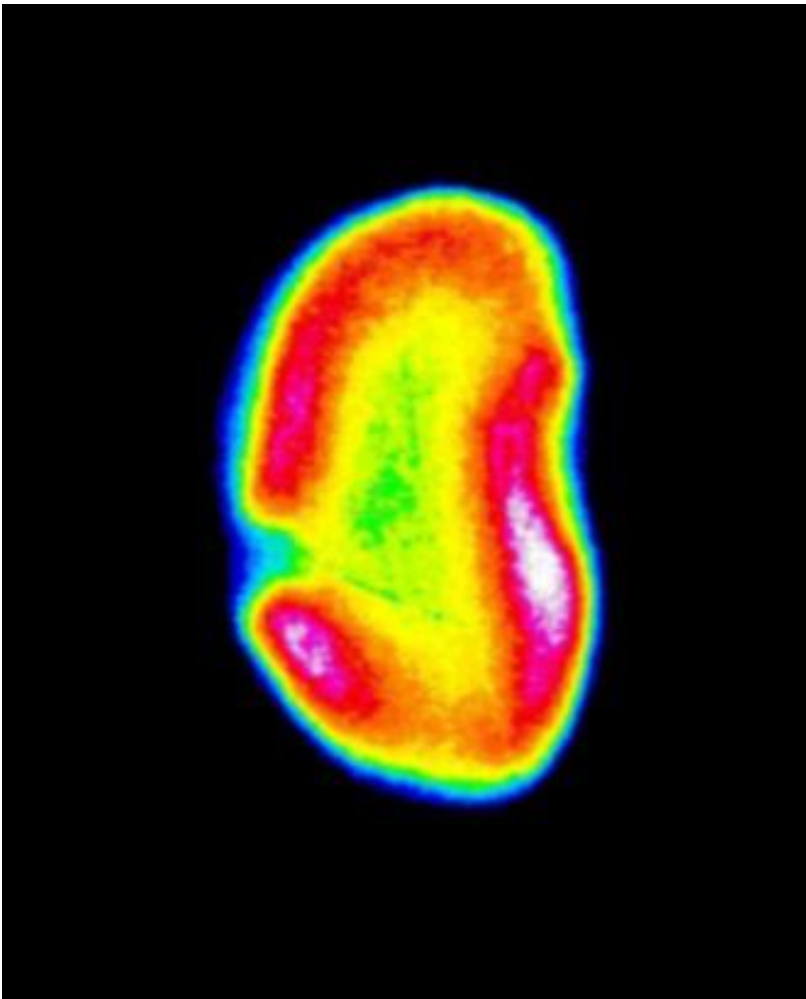


Figure 6

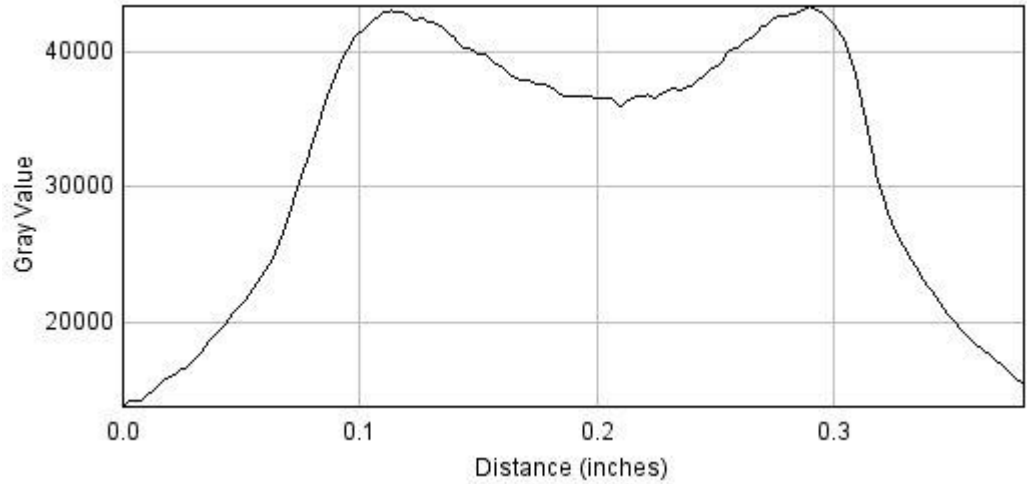


Figure 7

The Figure 8 is an autoradiography of the liver of a mouse injected with $^{188}\text{Re(V)}$ -DMSA; in this case it is clearly visible that no specific location or non uniformity of distribution of radioactivity can be identified, as demonstrated in Figure 9, that is a linear scan plot of the liver radioactivity along a line transverse to the organ.

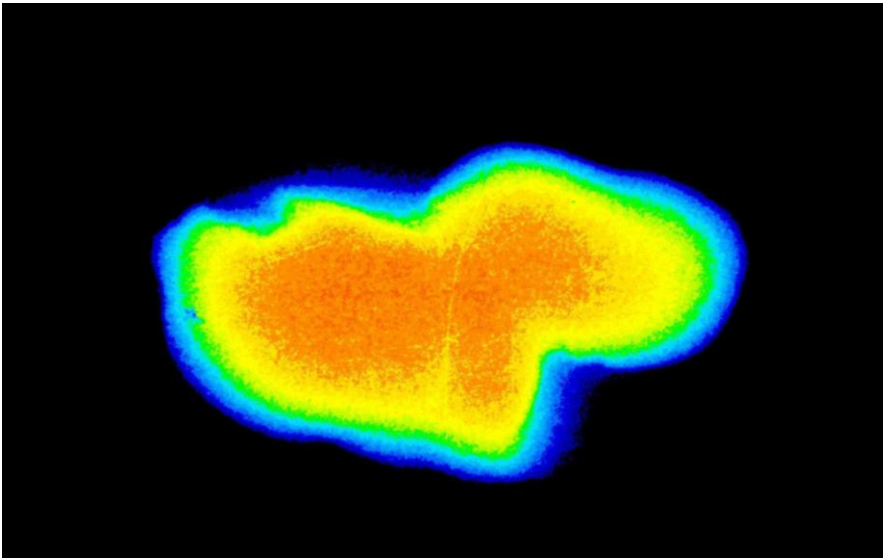


Figure 8

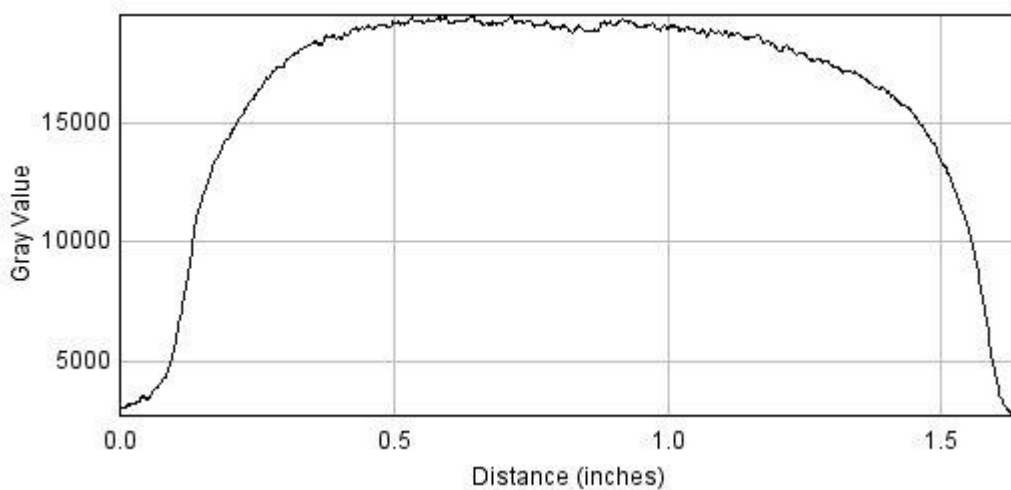


Figure 9

The Figure 10 is an autoradiography of a mouse femur injected with $^{188}\text{Re(V)}$ -DMSA; in spite of the low resolution of the scintigraphy, in this case the maximum concentration of radioactivity can be identified in the epiphyseal region of the femur.

Also Horiuchi-Suzuki et al. (32) have clearly demonstrated radioactivity localization of $^{186}\text{Re(V)}$ -DMSA in the epiphyseal growth plate of the femur. Enzymatic histochemistry also indicated that the area of accumulated radioactivity overlapped the area rich in osteoclast cells.

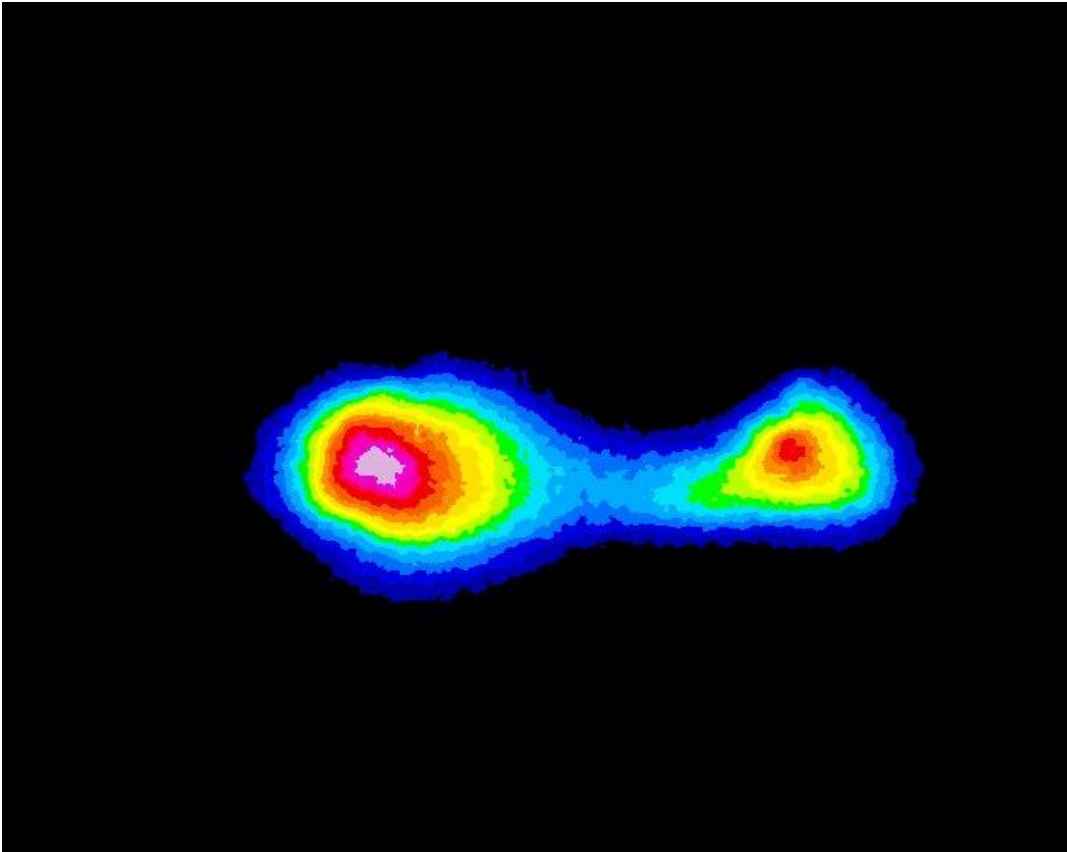


Figure 10

The Figure 11 shows a typical scintigraphic distribution of $^{188}\text{Re(V)}$ -DMSA; 300 microliters containing 1000 microCi of the tracer were injected in the ocular plexus, and scintigraphy was obtained 3 h after injection.

On 6 animals the specific ^{188}Re activity fixed on critical organs has been

<i>ORGAN</i>	<i>SPECIFIC RADIOACTIVITY (microCurie/g)</i>
kidneys	79 ± 5
liver	6 ± 2
femur	20 ± 3

By considering that the injected activity of ^{188}Re was has been more than three times the corresponding activity of the $^{99\text{m}}\text{Tc}$ tracer, we can easily calculate that the renal uptake by using $^{188}\text{Re(V)}$ -DMSA is higher of the corresponding uptake of $^{99\text{m}}\text{Tc(V)}$ -DMSA by less than 30%.

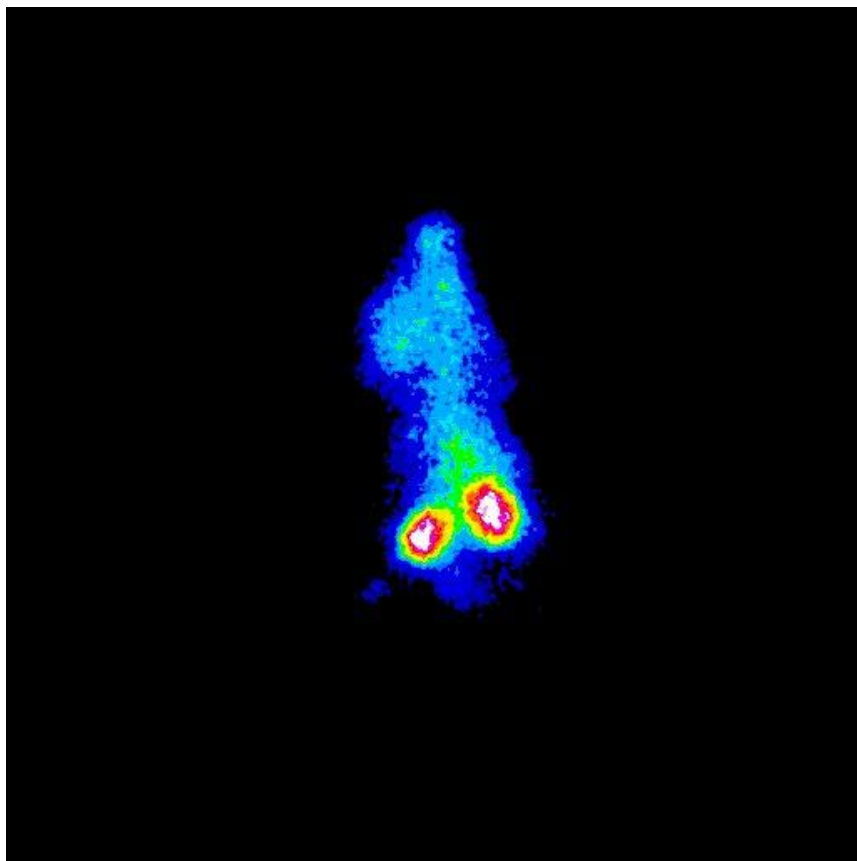


Figure 11

Discussion

As above reported (35), $^{188}\text{Re(V)}$ -DMSA showed selectivity for bone metastases and kidney, but uptake in normal bone was not significantly greater than in surrounding soft tissues; among the normal tissues the kidneys received the highest radiation dose (0.5–1.3 mGy/MBq). Since normal bone could not be distinguished from soft tissue on the scans, the calculated bone marrow doses (<0.1 mGy/MBq) did not differ greatly from the dose to the remainder of the body. It was estimated that with an injected activity of 7400 MBq, the renal radiation dose would not reach the minimum threshold of 1000 cGy, at which radiation nephritis is a risk.

External kidney irradiation causes progressive tissue injury that results in organ dysfunction and fibrosis. This process is an example of tissue response to radiation that may affect any organ exposed to therapeutic irradiation. Because kidney inflammation is minimal or absent upon radiation exposure, the term radiation nephritis, originally introduced to describe this clinical entity, has been progressively replaced with the more appropriate term radiation nephropathy.

The dose of radiation to which the kidneys are today exposed in patient undergoing bone marrow transplantation, is of the order of 10-12 Gy, lower than the doses traditionally associated with radiation nephropathy, which are usually greater than 2000 cGy. Luxton identified 2500 rads as the threshold dose for radiation nephropathy, but this dose was for irradiation spread out in multiple fractions over 25 to 30 days (37).

While the preliminary clinical data are quite promising, renal radiation dose might be a matter of concern in a possible high dose therapeutic clinical trial.

About this particular technique to decrease the renal uptake, both the above reported communication and the present paper can only be considered preliminary data, and still need an accurate confirmation, and a process of optimization in administration routes and kinetics uptake studies under different conditions. In spite of these limitations, their potential value can be considered quite promising. As above reported, the dose to kidneys can be considered the limiting factor in up-scaling the $^{188}\text{Re(V)}$ -DMSA for therapeutic purposes. The protocol for a start of a clinical trial aimed at the palliation of patients with dolorous bone metastases from prostatic cancer is in preparation.

The specific objectives to be achieved are:

Determination of the biodistribution of radiopharmaceuticals.

Identification of a dosimetric model that allows the determination of the dose to the critical organs and metastases after administration of the diagnostic radiopharmaceutical.

Preparation of guidelines for the determination of dosimetric estimation in patients with skeletal metastases.

Use in selected patients with bone metastases to be subjected to pain palliation.

Phase I: administration of the diagnostic dose of $^{99\text{m}}\text{Tc (V)}$ -DMSA scintigraphy and subsequent whole body scan. Quantitative evaluation of the compilation of

radiotracer

Phase II: administration of a tracer dose of ^{188}Re (V)-DMSA scintigraphy and subsequent whole body scan. Quantitative evaluation of the compilation of radiotracer. Comparison with the previous scintigraphy and accurate dosimetric evaluation.

Phase III: eventual administration of palliative dose / therapeutic ^{188}Re (V)-DMSA. Whole body scan on the day following administration.

Phase IV: periodic evaluation of the efficacy in terms of improvement of pain (VAS-visual analog scale, Wisconsin test, Karnofsky test, decreased consumption of analgesics, improvement of the general conditions, performance status and quality of life); periodic evaluation of hematologic toxicity.

References

1. Yokoyama A., Hata N., Horiuchi K., *et al.* (1985) The design of a pentavalent ^{99m}Tc-dimercaptosuccinate complex as a tumor imaging agent. *Int. J. Nucl. Med. Biol.* **12**, 273–279.
2. Clarke S., Lazarus C. and Maisey M. (1989) Experience in imaging medullary thyroid carcinoma using ^{99m}Tc (V) dimercaptosuccinic acid (DMSA). *Henry Ford Hosp. Med. J.* **37**(3-4), 167–168.
3. Hirano T., Otake H., Yoshida I. and Endo K. (1995) Primary lung cancer SPECT imaging with pentavalent technetium-^{99m}-DMSA, *J. Nucl. Med.* **36**, 202–207.
4. Ohta H., Endo K., Fujita T., *et al.* (1994) Imaging of soft tissue tumors with Tc(V)-^{99m} dimercaptosuccinic acid. A new tumor-seeking agent, *Clin. Nucl. Med.* **9**, 568–573.
5. Atasever T., Gundoglu C., Vural Ghapucu L.O., *et al.*, Evaluation of pentavalent ^{99m}Tc(V)DMSA scintigraphy in small cell and non small cell lung cancers, *Nuklearmedizin*, 1997, 337 (6): 223-227.
6. Watkinson J. C., Lazarus C. R., Mistry R., Shaheen O. H., Maisey M. N. and Clarke S. E. (1989) Technetium-^{99m} (V) dimercaptosuccinic acid uptake in patients with head and neck squamous carcinoma: experience in imaging, *J. Nucl. Med.* **30**, 174–180.
7. Hirano T., Otake H., Yashida I., *et al.*: Primary Lung Cancer SPECT imaging with Tc-^{99m} pentavalent DMSA, *J. Nucl. Med.*, 1995, 36: 202-7.
8. Wang S.J., Lin W.Y., Wey S.P., *et al.*: Pentavalent ^{99m}TcDMSA in imaging of hepatocellular carcinoma. *Neoplasia*, 1999, 46 (4): 246-248.
9. Mostafa H, Ebeid E, Zaher A, Shoukry N. Role of Tc-^{99m} MIBI and Tc-^{99m} DMSA-V in Evaluation of Bone Tumors. *Journal of the Egyptian Nat. Cancer Inst.*, Vol. 15, No. 2, June: 93-106, 2003.
10. Lam A, Blower PJ, Kettle AG, O'Doherty MJ, Coakley AJ. Pentavalent ^{99m}Tcm-DMSA in bone tumours: in vitro and in vivo studies [abstract]. *Nucl Med Commun* 1995; 16: 230.
11. Lam A.S., Kettle A.G., O'Doherty M.J.: Pentavalent ^{99m}Tc(V)DMSA imaging in bone metastases. *Nucl. Med. Comm.*, 1997, 18 (10): 1741-1749.
12. A.F.Sedda, G.Rossi, S.Shukla, G.Atzei, C.Cipriani, Fibrous dysplasia imaging with Tc-^{99m}(V)-DMSA, European Association of Nuclear Medicine- Annual Congress, Wien September 2002.

13. S.K.Shukla, G. Atzei, G.Argirò, P. Iannantuono, S. Boemi, G. Politano, A.F. Sedda, G. Rossi, C.Cipriani, Optimal ^{99m}Tc (V)-DMSA formulation for the diagnosis of cancer and of malignant or benign skeletal lesions, Italian Association of Nuclear Medicine-Genova 2002
14. Kobayashi S. H., Hosono M., Shirato M., *et al.* (1994) Soft-tissue tumors: Diagnosis with ^{99m}Tc (V) dimercaptosuccinic acid scintigraphy. *Radiology* **190**, 277–280.
15. Jemal, A., Murray, T., Samuels, A., Ghafoor, A., Ward, E. and Thun, M. J.: Cancer statistics, 2003. *CA Cancer J Clin*, **53**: 5, 2003.
16. Denoyer D, Perek N, Le Jeune N, Frere D, Dubois F (2004) Evidence that ^{99m}Tc-(V)-DMSA uptake is mediated by NaPi cotransporter type III in tumour cell lines. *Eur J Nucl Med Mol Imaging* 31: 77–84.
17. Blower PJ, Singh J, Clarke SE. The chemical identity of pentavalent technetium-^{99m}-dimercaptosuccinic acid. *J Nucl Med* 1991; 32:845–849.
18. Yokoyama A, Hata N, Horiuchi K, Masuda H, Saji H, Ohta H, Yamamoto K, Endo K, Torizuka K. The design of a pentavalent ^{99m}Tc-dimercaptosuccinate complex as a tumor imaging agent. *Int J Nucl Med Biol* 1985; 12:273–279.
19. Fatma J. Al-Saeedi, Princy M. Mathew, Yunus A. Luqmani, Assessment of Tracer ^{99m}Tc(V)-DMSA Uptake as a Measure of Tumor Cell Proliferation In Vitro, *PloS One*, January 2013 | Volume 8 | Issue 1
20. Kobayashi H, Shigeno C, Sakahara H, Hosono M, Hosono M, Yao ZS, Endo K, Konishi J., Intraosseous hemangiomatosis: technetium-^{99m}(V)dimercaptosuccinic acid and technetium-^{99m}-hydroxymethylene diphosphonate imaging. *J Nucl Med*. 1994 Sep;35(9):1482-4.
21. Athanasoulis T, Koutsikos J, Zerva C, What is the source of the skeletal affinity of ^{99m}Tc-V-DMSA, *Eur J Nucl Med Mol Imaging*. 2004 Dec;31(12):1673-4.
22. Glimcher MJ (2006) Bone: nature of the calcium phosphate crystals and cellular, structural, and physical chemical mechanisms in their formation. In: Sahai N, Schoonen MAA (eds) (2006), *Medical Mineralogy and Geochemistry*, vol 64. The Mineralogical Society of America, Chantilly, Virginia, pp 223–282.
23. Elliott JC (1994) *Structure and chemistry of the apatites and other calcium orthophosphates*. Elsevier, Amsterdam
24. Pellegrino ED, Blitz RM (1972) Mineralization in the chick embryo. I. Monohydrogen phosphate and carbonate relationships during maturation of the bone crystal complex. *Calif Tissue Res* 10:128–135

25. Biltz RM, Pellegrino ED (1977) The nature of bone carbonate. *Clin Orthop* 129:279–292
26. Legeros RZ (1994) Biological and synthetic apatites. In: Brown PW, Constanz B (eds) *Hydroxyapatite and related materials*. CRC, Boca Raton, pp 3–28.
27. C. Rey & C. Combes & C. Drouet & M. J. Glimcher, Bone mineral: update on chemical composition and structure, *Osteoporos Int* (2009) 20:1013–1021.
28. Bi X, Sterling JA, Merkel AR, Perrien DS, Nyman JS, Prostate cancer metastases alter bone mineral and matrix composition independent of effects on bone architecture in mice — A quantitative study using microCT and Raman spectroscopy, *Bone*, 56(2), 454–460.
29. Tannock I. F. and Rotin D. (1989) Acid pH in tumors and its potential for therapeutic exploitation. *Cancer Res.* **49**, 4373–84.
30. Lam ASK, Puncher MRB, Blower PJ. In vitro and in vivo studies with pentavalent technetium-99m dimercaptosuccinic acid. *Eur J Nucl Med* 1996; 23: 1575-1582.
31. Validated Biosystems Quarterly Resource Guide for Downstream Processing, Summer course 1998, Validated Biosystems, Inc., Tucson, Arizona USA 85750,
32. Horiuchi-Suzuki K, Konno A, Ueda M, Fukuda Y, Nishio S, Hashimoto K, Saji H, Skeletal affinity of Tc(V)-DMS is bone cell mediated and pH dependent, *European Journal of Nuclear Medicine and Molecular Imaging* Vol. 31, No. 3, March 2004
33. Lehenkari PP, Laitala-Leinonen T, Linna TJ, Vaananen HK, The regulation of pH_i in osteoclasts is dependent on the culture substrate and on the stage of the resorption cycle. *Biochem Biophys Res Commun* 1997; 235:838–844.
34. Blower PJ, Kettle AG, O'Doherty MJ, Coakley AJ, Knapp FF Jr., 99mTc(V)DMSA quantitatively predicts 188Re(V)DMSA distribution in patients with prostate cancer metastatic to bone. *Eur J Nucl Med* 2000; 27: 1405-1409.
35. Blower PJ, Lam ASK, O'Doherty MJ, Kettle AG, Coakley AJ, Knapp Jr FF, Pentavalent rhenium-188 dimercaptosuccinic acid for targeted radiotherapy: synthesis and preliminary animal and human studies, *Eur J Nucl Med* (1998) 25:613–621
36. Houston S, Allen S, Lazarus CR, et al. Modifying renal uptake of pentavalent 99mTcDMSA and 186Re DMSA offers potential for tumour targeted radiotherapy of medullary thyroid carcinoma (MTC). *Nucl Med Commun* 1992;13:211.
37. Luxton, RW: Radiation nephritis. *Q J Med* 1953 22: 215–242.

Edito dall' **ENEA**
Servizio Comunicazione

Lungotevere Thaon di Revel, 76 - 00196 Roma

www.enea.it

Stampa: Tecnografico ENEA - CR Frascati
Pervenuto il 30.9.2014

Finito di stampare nel mese di ottobre 2014